

Errors of Molecular Dynamics Simulations, and “Accurate” Al-Cu-H and Mg-H Potentials

X. W. Zhou, R. B. Ryan, D. K. Ward, R. A. Karnesky, M. E. Foster,
V. Stavila, M. D. Allendorf

Sandia National Laboratories

T. W. Heo, B. C. Wood, S. Kang

Lawrence Livermore National Laboratories

Sandia National Laboratories is a multi-mission laboratory managed and operated by National Technology and Engineering Solutions of Sandia, LLC., a wholly owned subsidiary of Honeywell International, Inc., for the U.S. Department of Energy’s National Nuclear Security Administration (NNSA) under contract DE-NA-0003525. Lawrence Livermore National Laboratory is operated for the US Department of Energy under Contract DE-AC52-07NA27344. The authors gratefully acknowledge research support from the U.S. Department of Energy, Office of Energy Efficiency and Renewable Energy, Fuel Cell Technologies Office, under Contract Numbers DE-AC04-94AL85000 and DE-AC52-07NA27344. Discussions with J. A. Zimmerman, N. Bartelt, R. Sills, D. Robinson, and D. Cowgill are also highly appreciated.

The views, opinions, findings, and conclusions stated herein are those of the authors and do not necessarily reflect those of CRDF Global, or the United States Government or any agency thereof. Neither the United States Government nor any agency thereof, nor any of their employees, makes any warranty, expressed or implied, or assumes any legal liability or responsibility for the accuracy, completeness, or usefulness of any information, apparatus, product, or process disclosed, or represents that its use would not infringe privately owned rights.



Outline

1. Statistical errors of molecular dynamics models
 - Dislocation energy calculations
 - Diffusivities calculations
2. Al-Cu-H bond order potential and its stability validation
3. Mg-H bond order potential and its stability validation



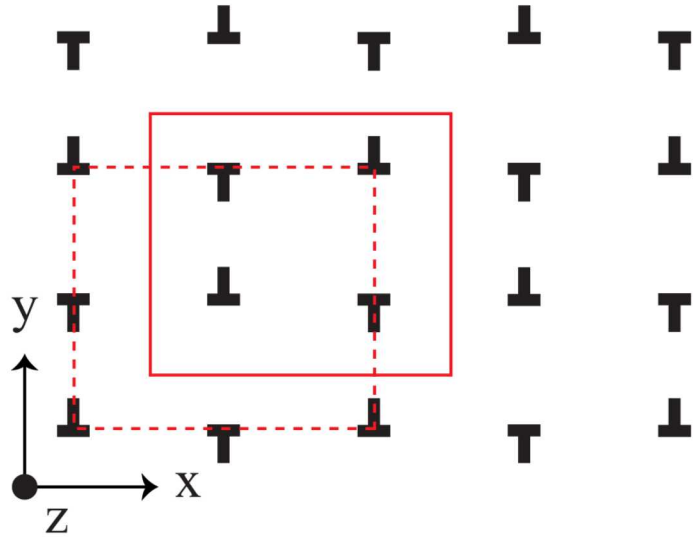
Continuum and Periodic Boundary Conditions

1. Dislocation cores must be calculated from atomistics, with boundary conditions addressing long range strain fields
2. One way is to fix the boundary atoms to the continuum solutions
 - Dislocation type unknown
 - Anisotropic calculations required
 - Boundary atoms for dislocated and perfect systems non-identical
3. Another way is to use periodic boundary conditions
 - Dislocation type accurately captured
 - Continuum calculations not required
 - Boundary atoms for dislocated and perfect systems consistent
 - No approximation is introduced regardless dislocation array configuration

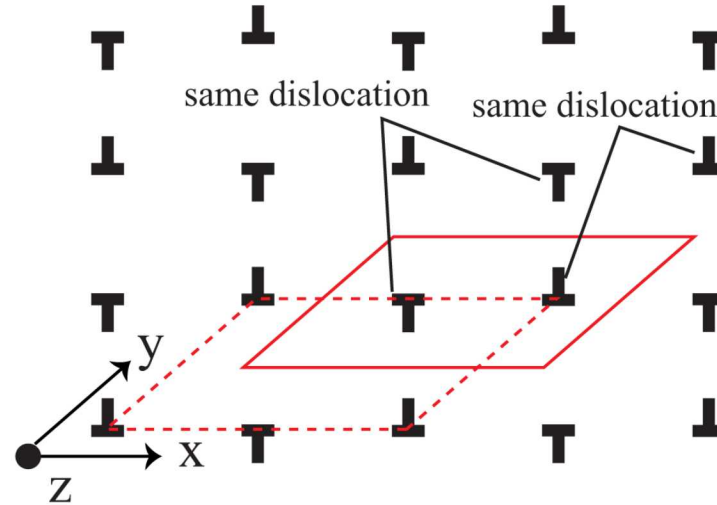


History of Periodic Methods

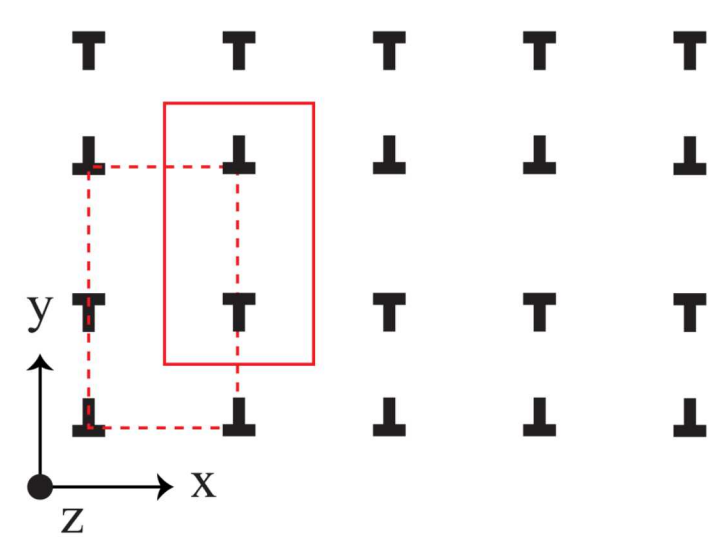
(a) Orthogonal cell requiring 4 dislocations



(b) Oblique cell requiring 2 dislocations



(c) Orthogonal cell requiring 2 dislocations



1. Traditionally quadruple dislocations shown in the left image are used (Bigger et al, PRL, 1992, 69, 2224)
 - Dislocations may annihilate
2. Quadruple dislocations can be implemented with oblique cell in the middle image
 - Literature only acknowledges the computational efficiency
 - Annihilation is more difficult
3. Single dipole configurations in the right image eliminate annihilation
 - Used successfully by Cai et al (e.g., PRL, 2001, 86, 5727)
 - Also successfully used by us

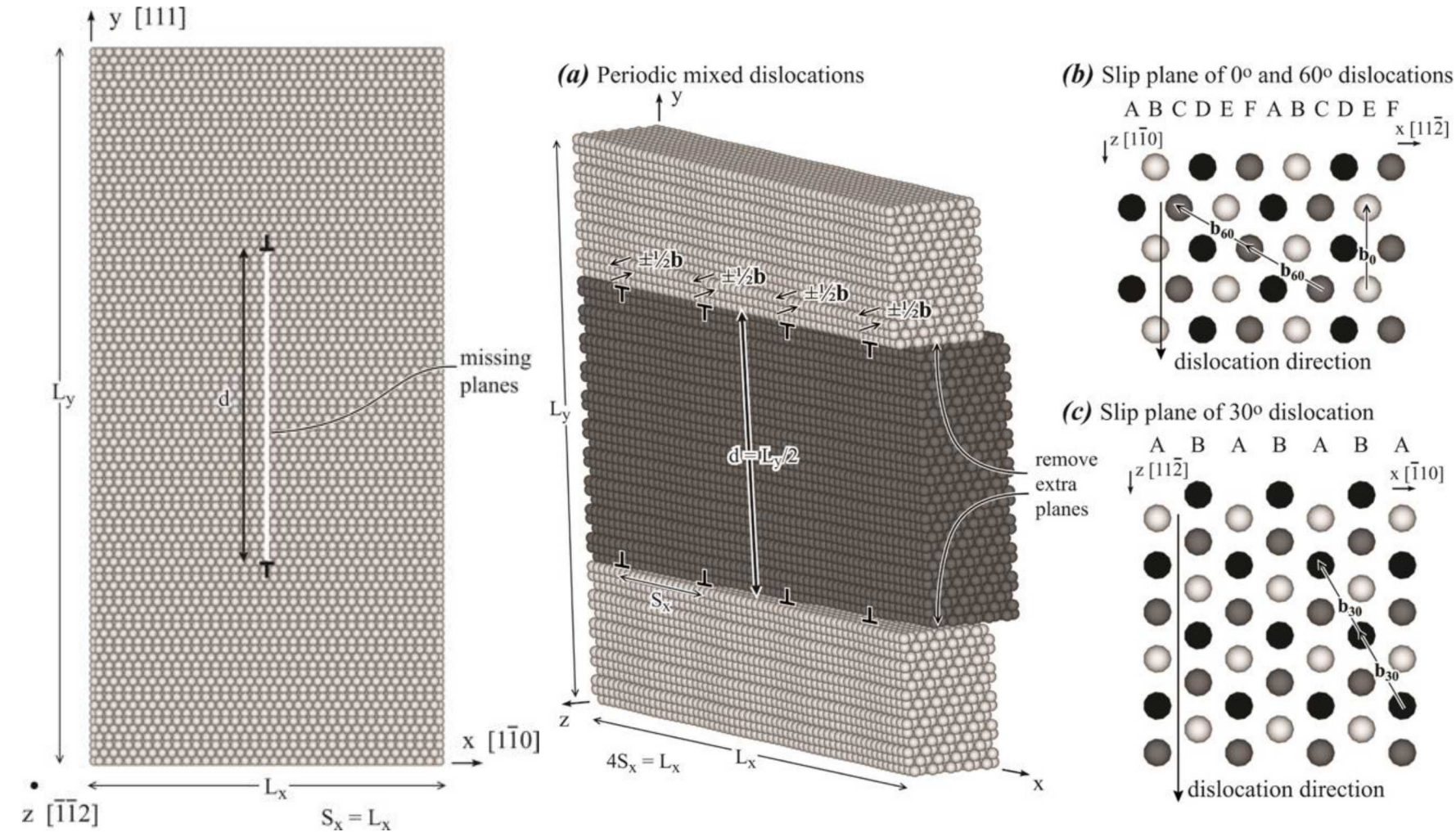


Our Unique Method

1. Method of periodic boundary conditions with only one dipole is not clear in Cai et al's papers
2. There is a conditional convergence problem in Cai et al's configuration
 - Experts' experiences are required to deal with this
3. Literature methods are limited by statistical errors
4. Our methods (Zhou et al, PRB, 2017, 95, 054112; JMPS, 2016, 91, 265; Uncertainty Quantification and Model Calibration, INTECH, Rijeka, Croatia, 2017) solved all the three problems above
 - Methods of periodic boundary conditions are simple and are described
 - Analytical expression for dislocation dipole arrays are derived
 - Time-averaged molecular dynamics reduces statistical errors



Dislocation Geometry

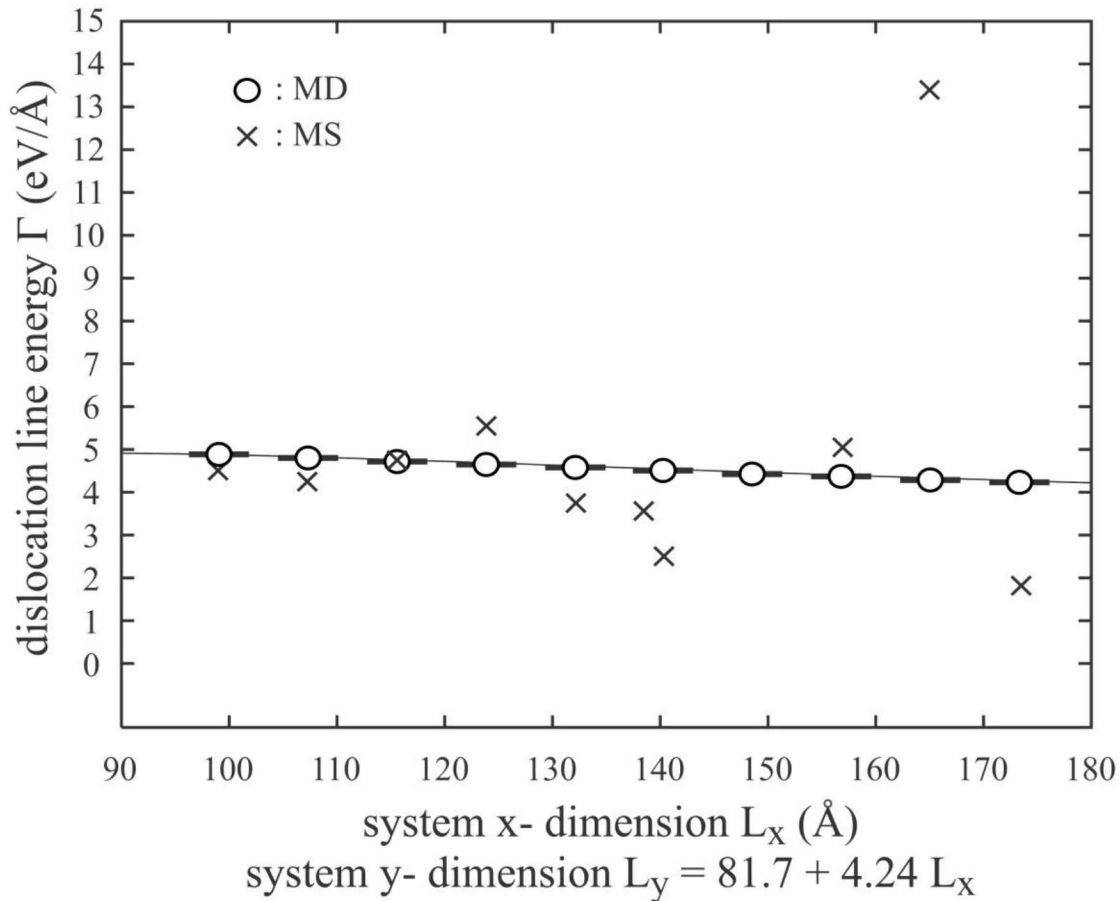


1. One dipole for edge dislocations
2. Multiple dipoles for other dislocations
3. Orthogonal cell can be used
4. Orthogonal cell, however, requires that $d = L_y/2$ for non-edge dislocations



Time-Averaged MD Calculations

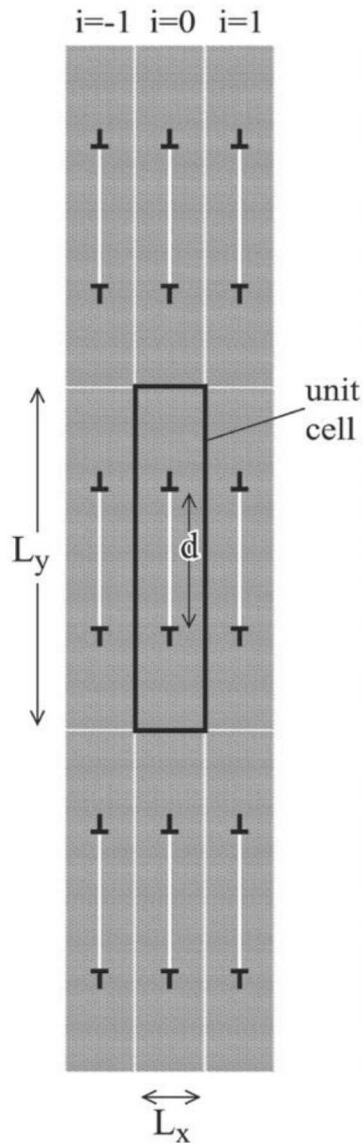
CdS Dislocation Energy



1. All literature calculations use molecular statics simulations at zero K
2. No literature calculations use big cells
3. We found that statistical errors of molecular statics simulations are too large for large systems (X. Zhou, and S. M. Foiles, in “Uncertainty Quantification and Model Calibration”, Ed. J. P. Hessling, p. 89 (INTECH, Rijeka, Croatia, 2017))
4. Time-averaged molecular dynamics can reduce statistical errors



Continuum Energy Expression



$$\Gamma = E_c + \frac{Gb^2}{4\pi(1-\nu)} \cdot \cos^2 \alpha + \sin^2 \beta \cdot E_{0,edge} + \cos^2 \beta \cdot E_{0,screw} + 2 \sin^2 \beta \cdot \sum_{i=1}^{\infty} E_{i,edge} + 2 \cos^2 \beta \cdot \sum_{i=1}^{\infty} E_{i,screw}$$

$$E_{0,edge} = \frac{Gb^2}{4\pi(1-\nu)} \left\{ \ln\left(\frac{d}{r_0}\right) + \ln\left(\frac{L_y - d}{L_y}\right) - \ln\left[Ga\left(\frac{L_y + d}{L_y}\right)\right] - \ln\left[Ga\left(2 - \frac{d}{L_y}\right)\right] \right\}$$

$$E_{0,screw} = \frac{Gb^2}{4\pi} \left\{ \ln\left(\frac{d}{r_0}\right) + \ln\left(\frac{L_y - d}{L_y}\right) - \ln\left[Ga\left(\frac{L_y + d}{L_y}\right)\right] - \ln\left[Ga\left(2 - \frac{d}{L_y}\right)\right] \right\}$$

$$E_{i,edge} = \frac{Gb^2}{8\pi(1-\nu)} \left\{ \frac{4\pi \cdot i \cdot L_x \cdot \coth\left(\frac{\pi \cdot i \cdot L_x}{L_y}\right) \cdot \sin^2\left(\frac{\pi \cdot d}{L_y}\right)}{L_y \cdot \cosh\left(\frac{2\pi \cdot i \cdot L_x}{L_y}\right) - L_y \cdot \cos\left(\frac{2\pi \cdot d}{L_y}\right)} + \ln\left[\cos^2\left(\frac{\pi \cdot d}{L_y}\right) + \coth^2\left(\frac{\pi \cdot i \cdot L_x}{L_y}\right) \cdot \sin^2\left(\frac{\pi \cdot d}{L_y}\right)\right] \right\}$$

$$E_{i,screw} = \frac{Gb^2}{8\pi} \ln\left[\cos^2\left(\frac{\pi \cdot d}{L_y}\right) + \coth^2\left(\frac{\pi \cdot i \cdot L_x}{L_y}\right) \cdot \sin^2\left(\frac{\pi \cdot d}{L_y}\right)\right]$$

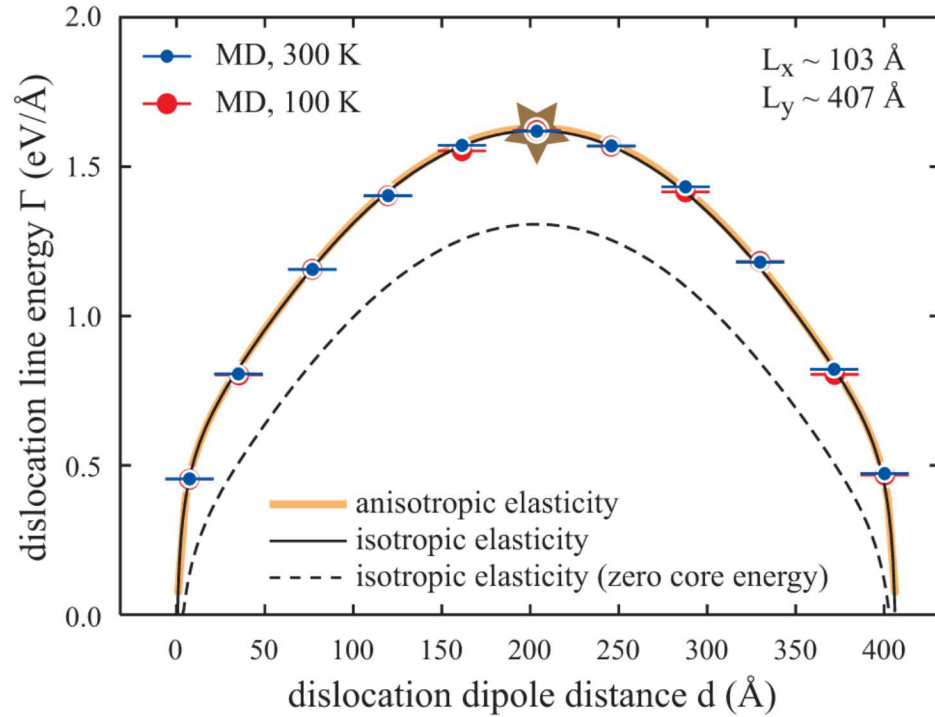
E_c independent of geometry!

- E_c, r_0 : core energy, radius
- Ga : Euler gamma function
- \coth, \cosh : hyperbolic functions
- G, ν : shear modulus, Poisson's ratio
- b : Burgers magnitude
- α : dislocation dipole direction ($\alpha = 0^\circ$ means vertical dislocation dipole)
- β : dislocation character angle

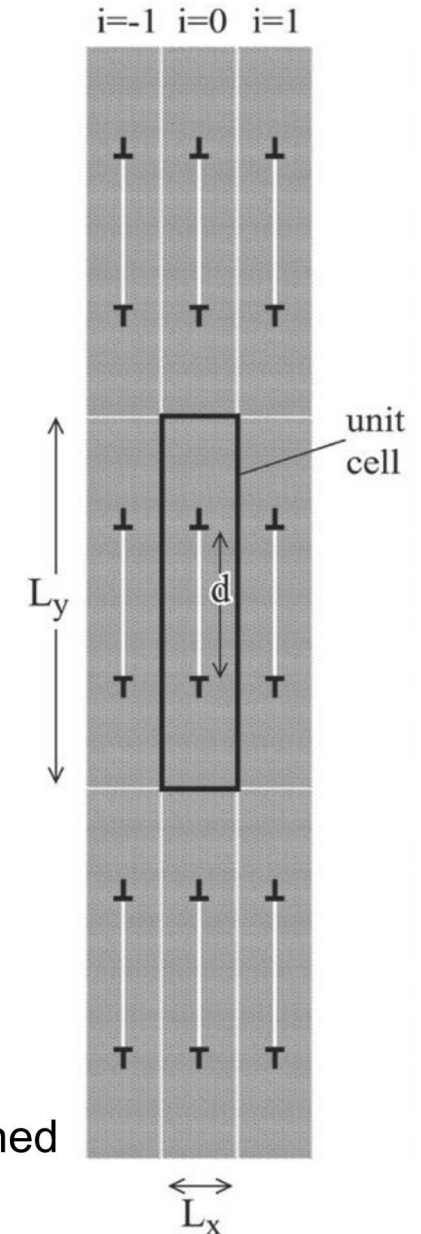
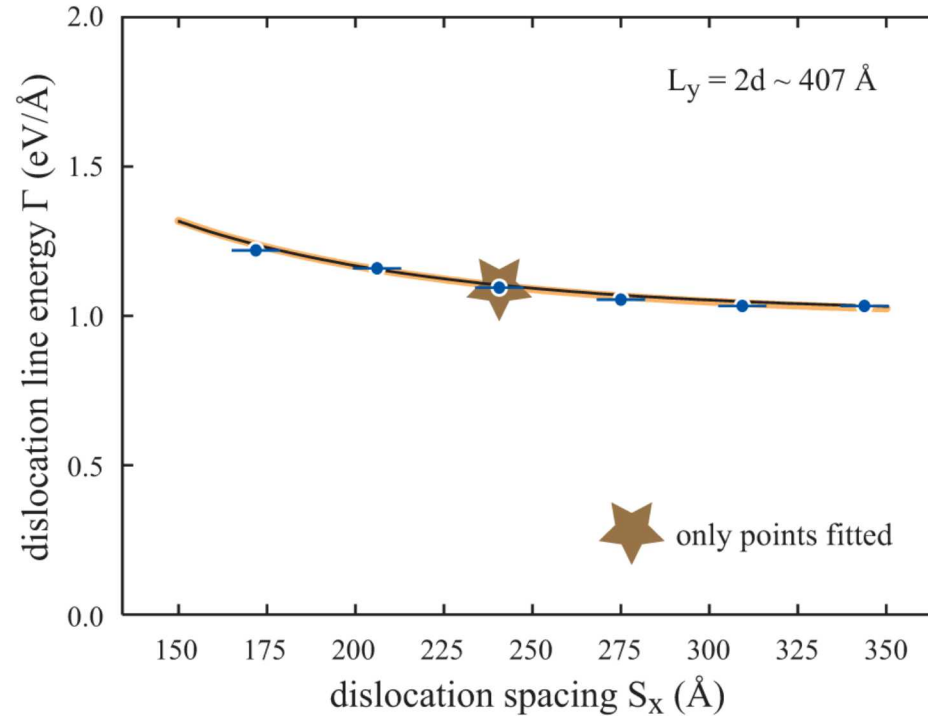


Edge Dislocation Results

(a) Effect of dislocation dipole distance d



(b) Effect of dislocation spacing $S_x (= L_x)$

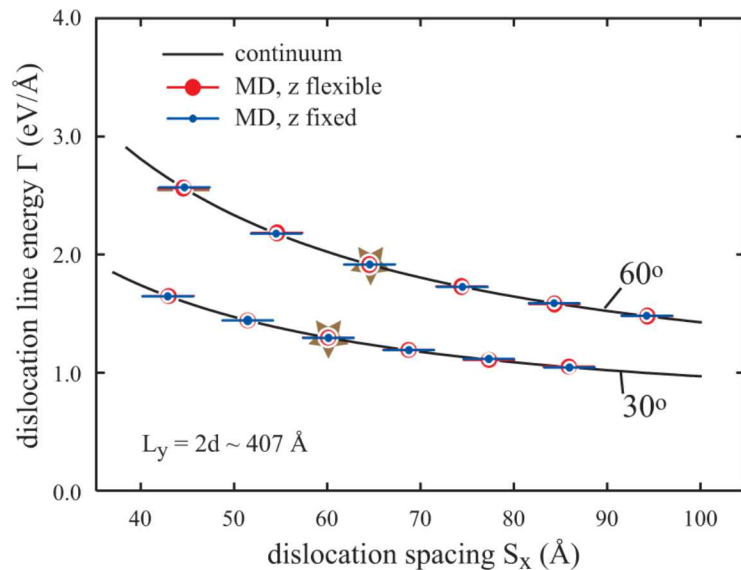


1. Continuum dislocation energy = $\Gamma(G, \nu, b, r_0, E_c, \beta, d, L_x, L_y)$
2. Simulations provide Γ values at a variety of (β, d, L_x, L_y)
3. Dislocation core radius r_0 can be any value as long as the energy within r_0 is captured by the E_c
4. By fitting the MD Γ values to the continuum expression at a chosen r_0 , (G, ν, E_c) can all be determined
5. Γ is a symmetric function of d (important to validate)

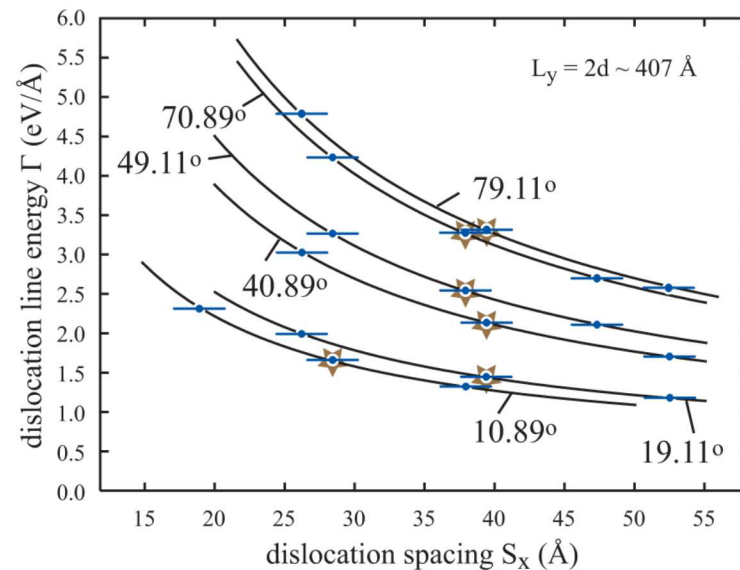


Mixed and Screw Dislocation Results

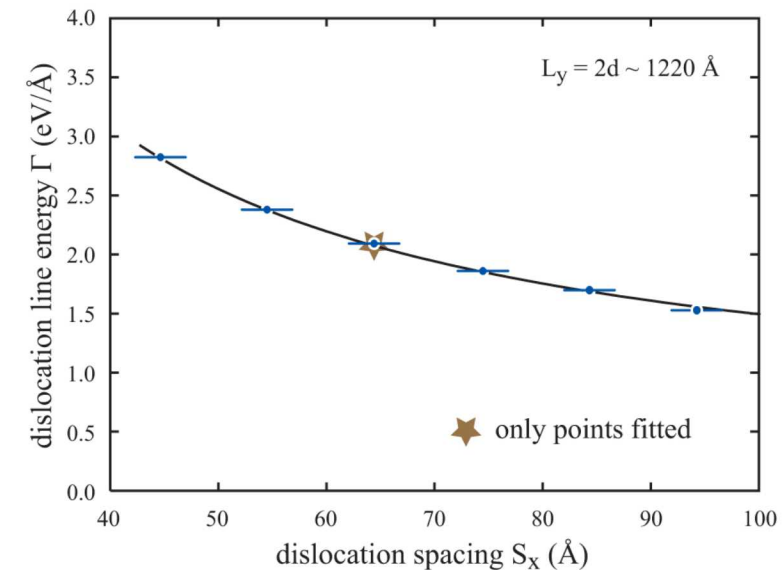
(a) 30°, 60° dislocations



(b) 10.89°, 19.11°, 40.89°, 49.11°, 70.89°, 79.11° dislocations



(c) 0.0° (screw) dislocation



1. There are only $N+2$ unknowns, (E_c at the N β angles + $G + v$), but many more equations
2. All MD data points have zero error bars
3. All MD data points fall exactly on continuum lines



Diffusion Analysis Methods

Molecular statics simulation of individual atomic jump path no longer works

1. The coordinates $\alpha_i(t)$ of N diffusion atoms ($i = 1, 2, \dots, N$), are recorded on a time interval of Δt , i.e., at times of $t = j\Delta t$, $j = 1, 2, \dots, m$ ($m = t_{\text{MD}}/\Delta t$), where Δt can be any multiple of the time step size dt used in the MD simulations.

2. $m+1-k$ measurements can be made for the displacement of a diffusion atom i over a $k\Delta t$ period: $\Delta\alpha_{i,j}(k\Delta t) = \alpha_i(j\Delta t - \Delta t + k\Delta t) - \alpha_i(j\Delta t - \Delta t)$ where $j = 1, 2, \dots, m+1-k$.

3. This allows us to calculate mean square displacement (MSD):

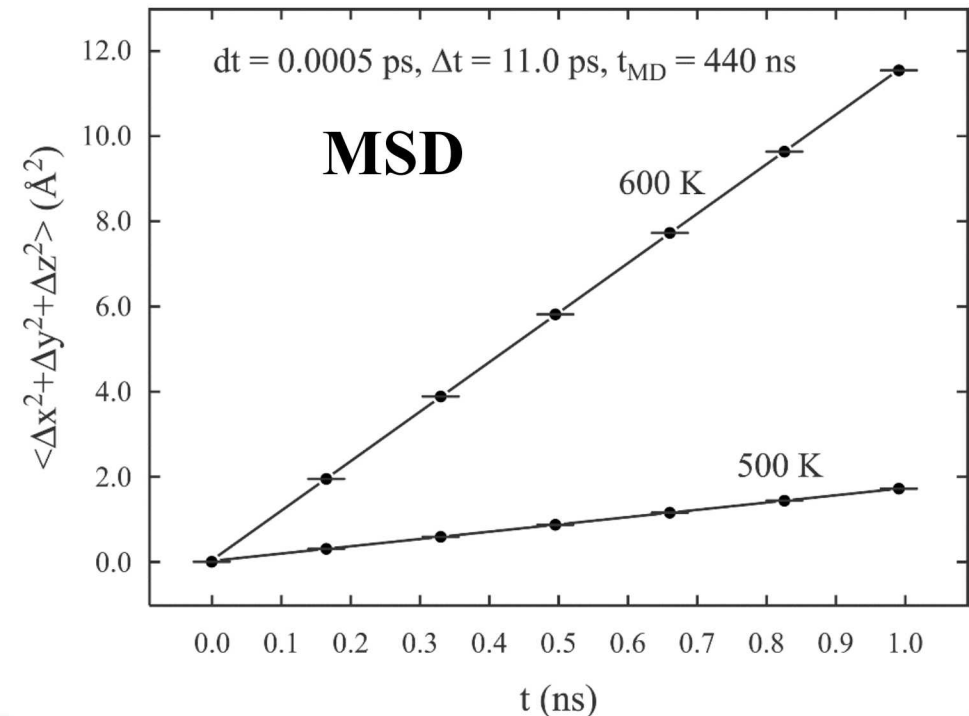
$$\langle [\Delta\alpha(k\Delta t)]^2 \rangle = \frac{\sum_{i=1}^N \sum_{j=1}^{m+1-k} [\Delta\alpha_{i,j}(k\Delta t)]^2}{N(m+1-k)}$$

4. MSD can be fitted to diffusivities D :

$$\langle [\Delta\alpha(k\Delta t)]^2 \rangle = 2D_\alpha t$$

$$\langle [\Delta x(k\Delta t)]^2 \rangle + \langle [\Delta z(k\Delta t)]^2 \rangle = 4D_{xz} t$$

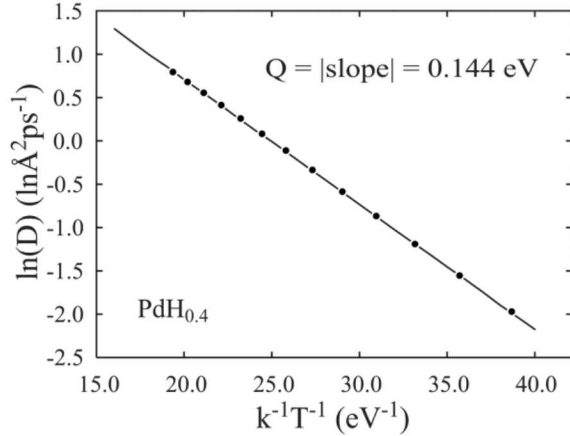
$$\langle [\Delta x(k\Delta t)]^2 \rangle + \langle [\Delta y(k\Delta t)]^2 \rangle + \langle [\Delta z(k\Delta t)]^2 \rangle = 6D_{xyz} t$$



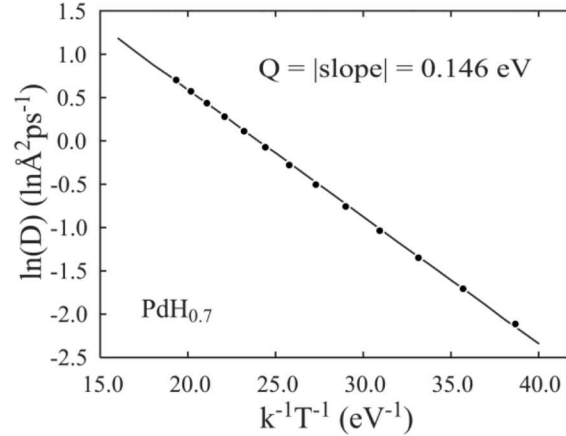
Pd-H Arrhenius Plots

$$t_{MD} = 2.2 \text{ ns}$$

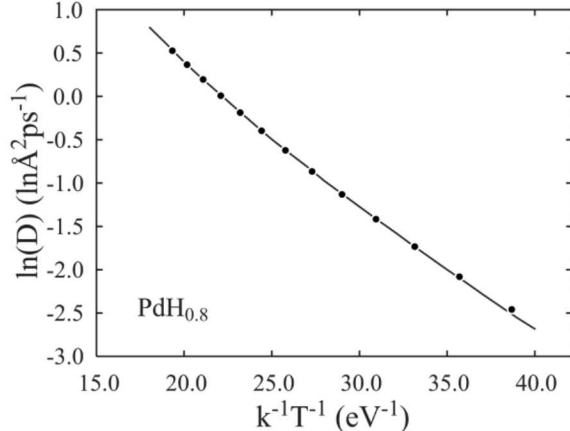
(a) hydrogen composition $x = 0.4$



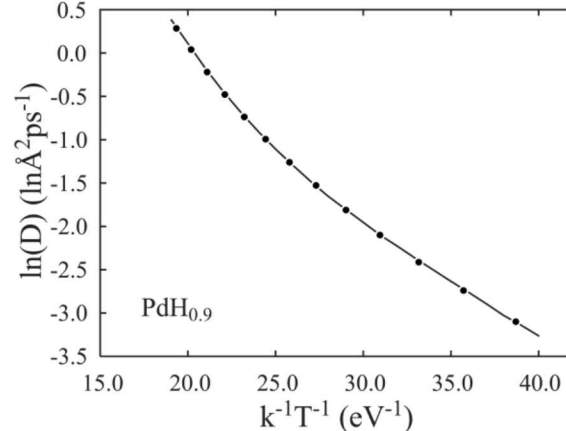
(b) hydrogen composition $x = 0.7$



(c) hydrogen composition $x = 0.8$



(d) hydrogen composition $x = 0.9$



1. MD results fall exactly on smooth lines
2. Statistical errors are negligible
3. The MD does not have time and length scale issues
4. The Arrhenius relation is satisfied at low H concentrations
5. The $\ln(D)$ vs. $1/T$ relation becomes non-linear at high H concentrations

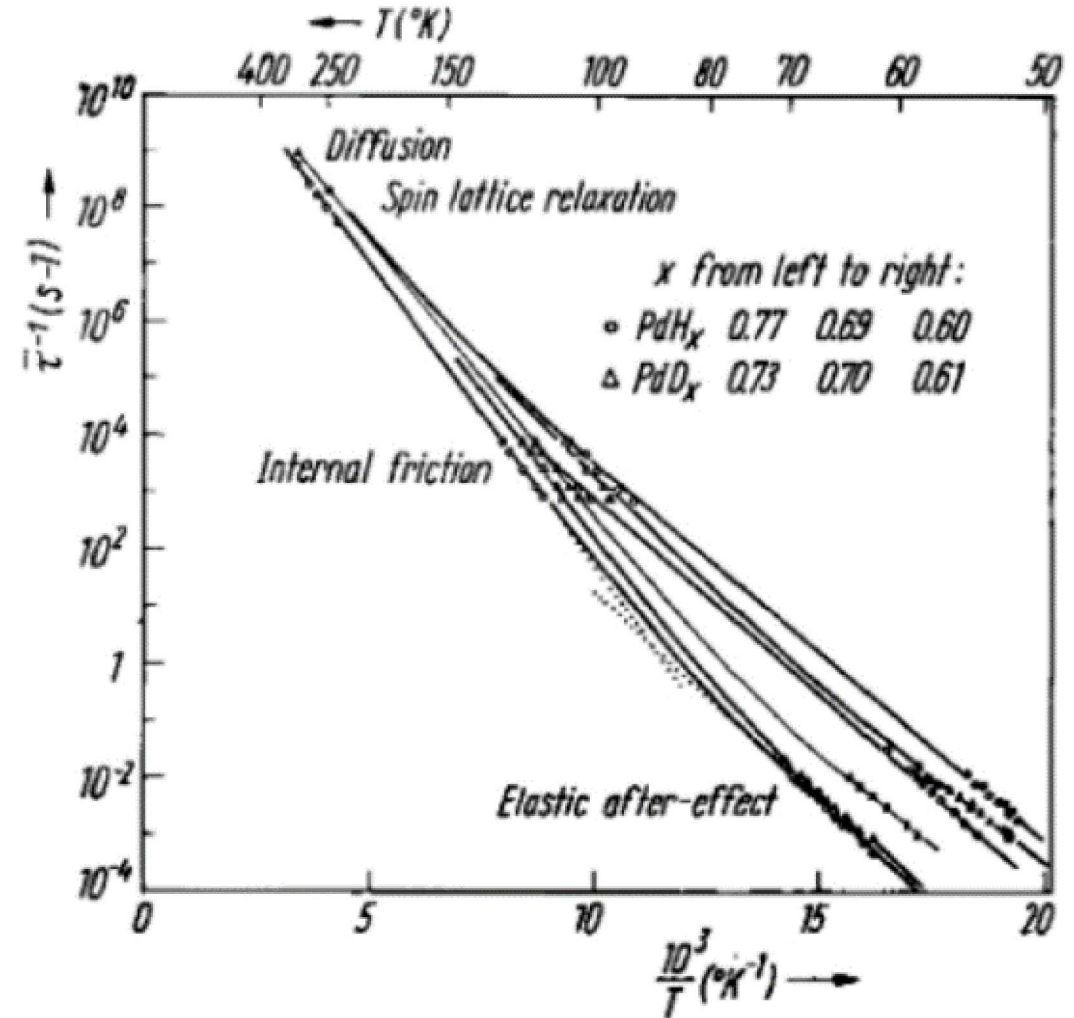


Table I. Measured and predicted activation energy Q and pre-exponential factor D₀ as a function of phase and temperature.

Authors	Phase	T (K)	Q (eV)	D ₀ (Å ² /ps)
Arons et al [2,3]	β	110-300	0.210	---
		50-100	0.150	---
Cornell et al [4]	β	195-300	0.228	---
		100-195	0.100	---
Mazzolai et al [5]	β	250-270	0.210	---
		130-200	0.130	---
Burger et al [6]	β	230-320	0.210	---
		180-230	0.060	---
Torrey et al [7]	β	>220	0.240	---
		<220	0.080	---
Beg et al [15]	β	293-473	0.146	1.10×10 ¹
Seymour et al [16]	β	296-413	0.229	9.30×10 ⁰
Davis et al [17]	β	300-400	0.228	3.00×10 ¹
Majorowski et al [18]	β	208-338	0.287	1.13×10 ²
Bucur [19]	α	278-323	0.054	2.48×10 ¹
Holleck [20]	α	533-913	0.055	2.94×10 ¹
Simmons et al [21]	α	273-650	0.062	6.10×10 ¹
Maeda et al [22]	α	773-1373	0.215	2.80×10 ¹
Hara et al [23]	α	523-773	0.219	2.40×10 ¹
Pietrzak et al [24,25]	α	273-473	0.230	2.20×10 ¹
Yoshihara et al [26]	α	273-350	0.231	2.91×10 ¹
Zuchner [27]	α	200-700	0.250	5.25×10 ¹
MD fitted Eqs. (1) - (5)	α	300-600	~0.15	~3.5×10 ¹
	β (x=0.8)	600	~0.20	~7.8×10 ¹
	β (x=0.8)	300	~0.14	~1.7×10 ¹

Review by X. W. Zhou et al, submitted

Experimental Validation

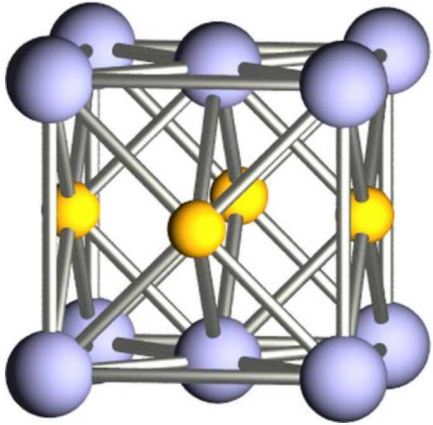


From Arons et al

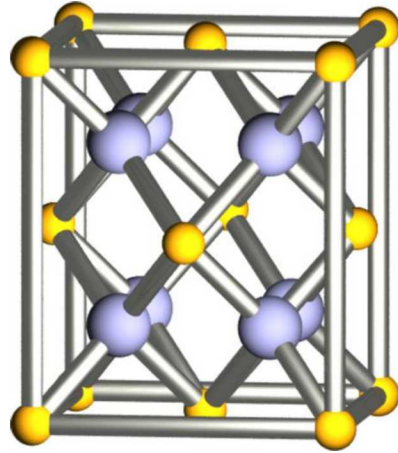


Challenging Atomistic Models

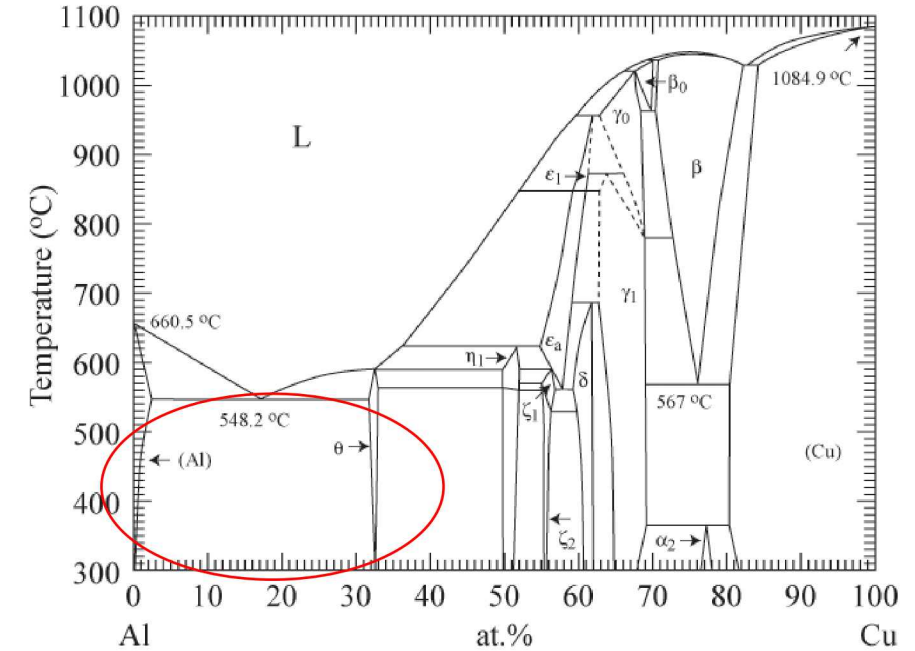
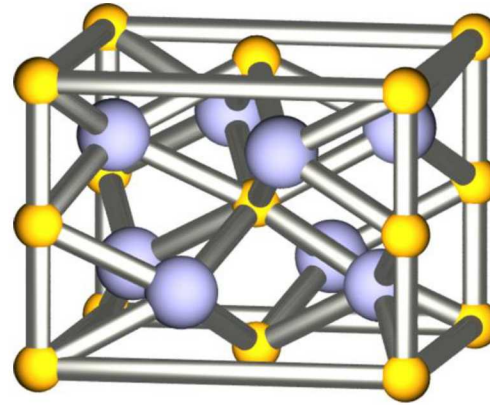
fcc (Al, Cu, GP zone)



θ' (Al_2Cu)



θ (Al_2Cu)

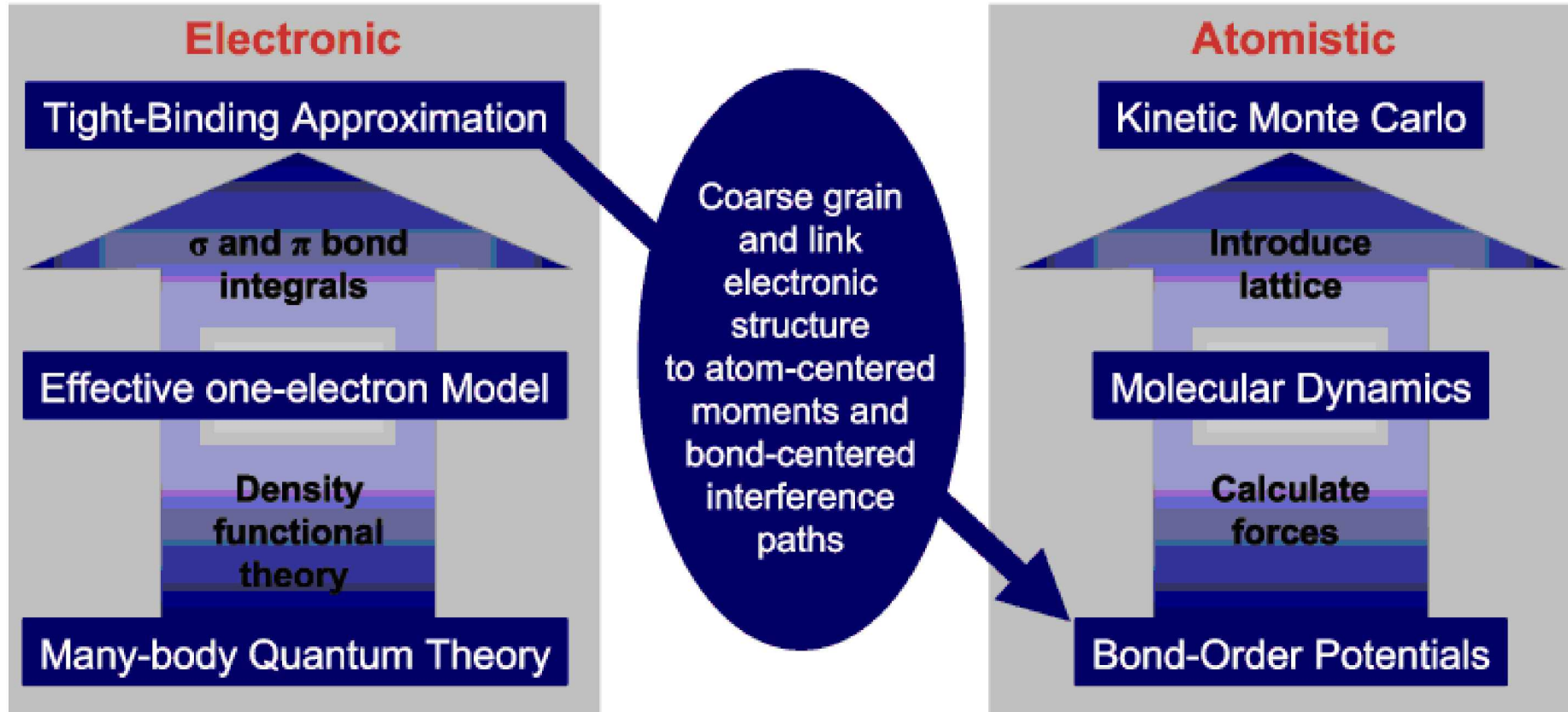


Can Model Even Captures These Crystals Structures?

1. Model must incorporate Al_2Cu phases to predict the precipitate-strengthening effects
2. θ and θ' Al_2Cu compounds are the most important
3. Precipitate formation: GP zone \rightarrow θ' (CaF_2) \rightarrow θ (Al_2Cu)



Analytical Bond Order Potential



D. G. Pettifor, M. W. Finnis, D. Nguyen-Manh, D. A. Murdick, X. W. Zhou, and H. N. G. Wadley, *Mater. Sci. Eng. A*, 365, 2 (2004).

D. G. Pettifor, and I. I. Oleinik, *Phys. Rev. B*, 59, 8487 (1999).

D. G. Pettifor, and I. I. Oleinik, *Phys. Rev. Lett.*, 84, 4124 (2000).

D. G. Pettifor, and I. I. Oleinik, *Phys. Rev. B*, 65, 172103 (2002).

R. Drautz, D. Nguyen-Manh, D. A. Murdick, X. W. Zhou, H. N. G. Wadley, and D. G. Pettifor, *TMS Lett.*, 1, 31 (2004).

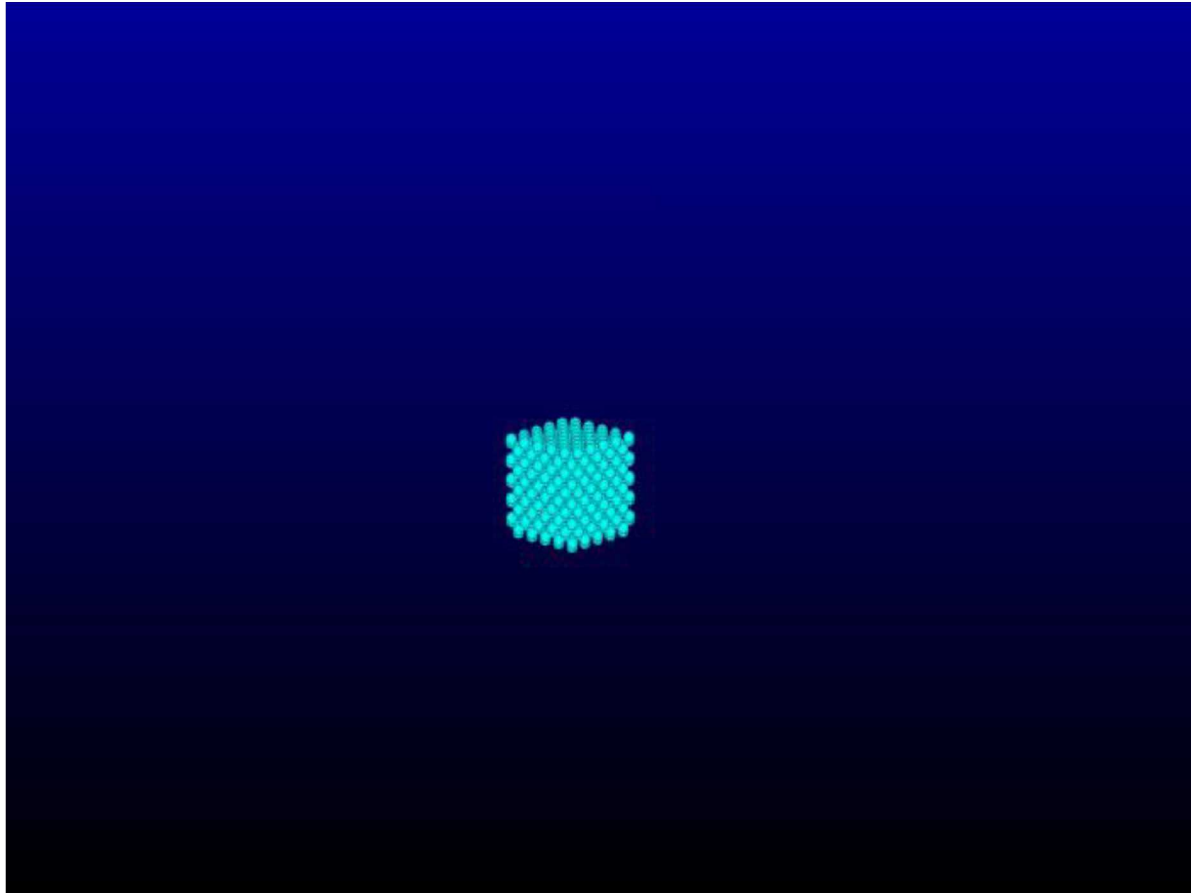
R. Drautz, D. A. Murdick, D. Nguyen-Manh, X. W. Zhou, H. N. G. Wadley, and D. G. Pettifor, *Phys. Rev. B*, 72, 144105 (2005).

D. A. Murdick, X. W. Zhou, H. N. G. Wadley, D. Nguyen-Manh, R. Drautz, and D. G. Pettifor, *Phys. Rev. B*, 73, 45206 (2006).

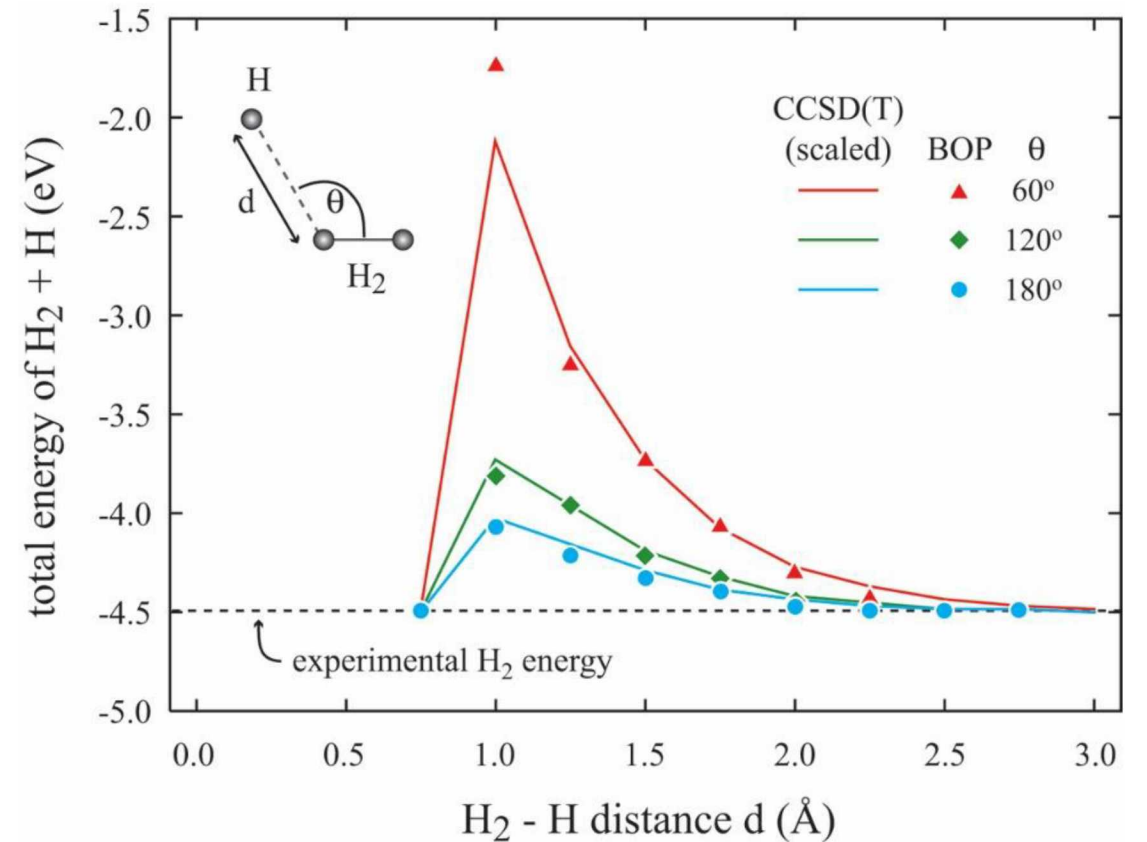


H- Component of the Potential

Hydrogen Crystal to H₂ Gas



H₂+H→H+H₂ Energy Profiles



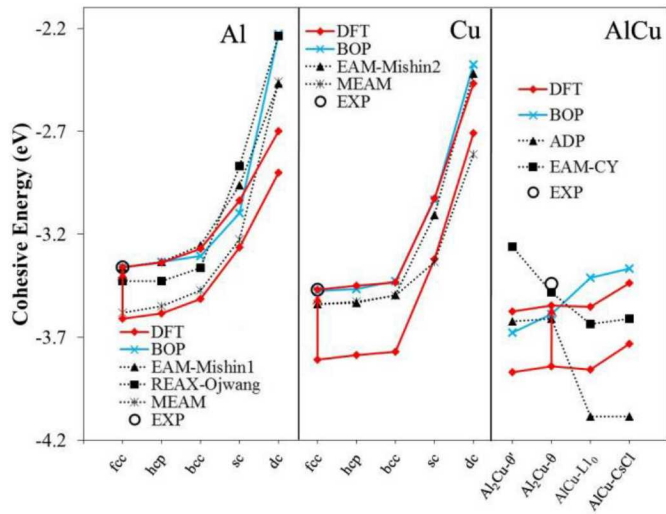
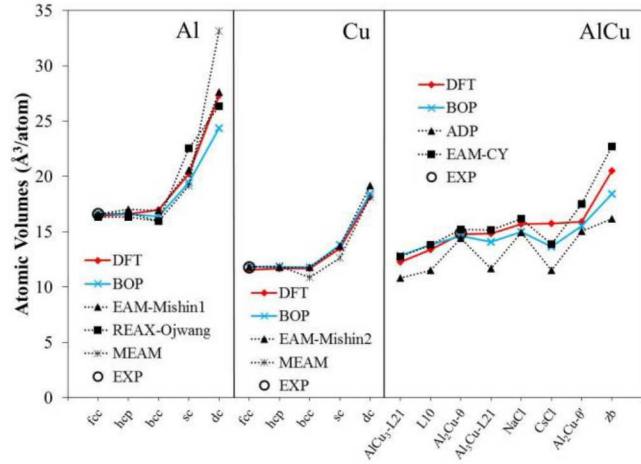
X. W. Zhou, D. K. Ward, M. Foster, J. A. Zimmerman, J. Mater. Sci., 50, 2859 (2015).



Energy and Volume Trends

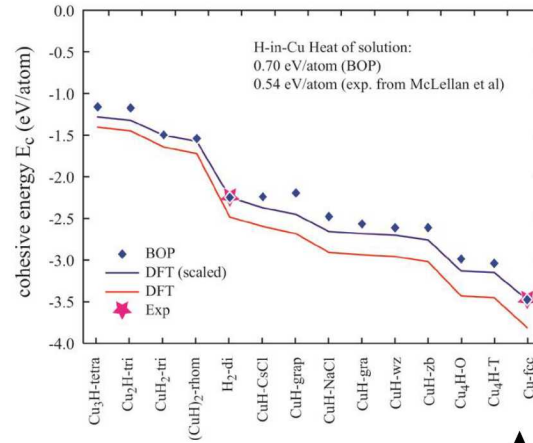
Heat of Solution

Al-Cu

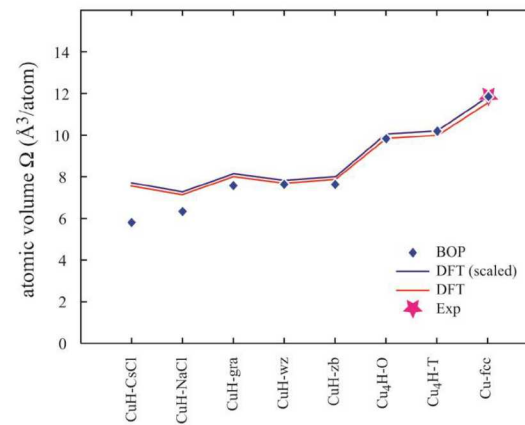


Cu-H

(a) cohesive energy per atom

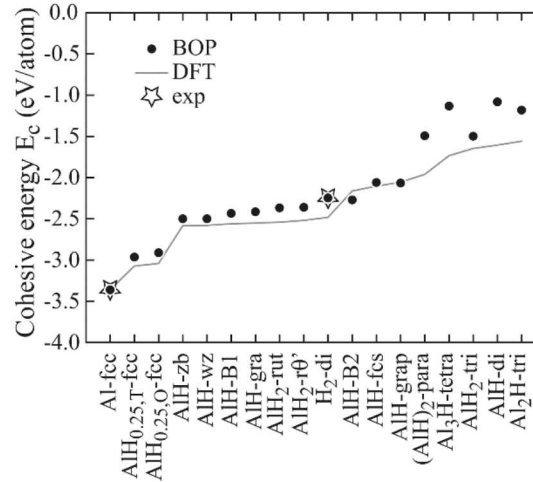


(b) atomic volume

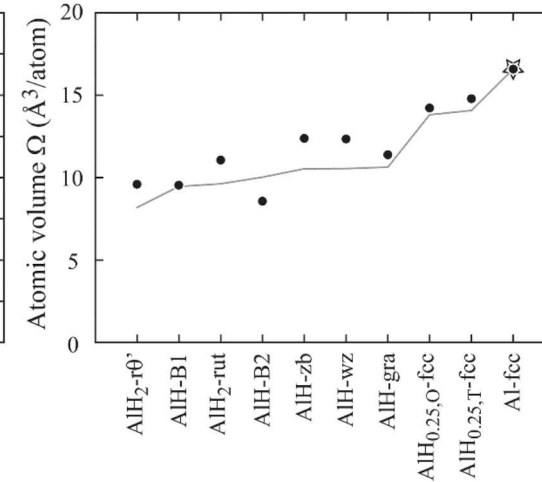


Al-H

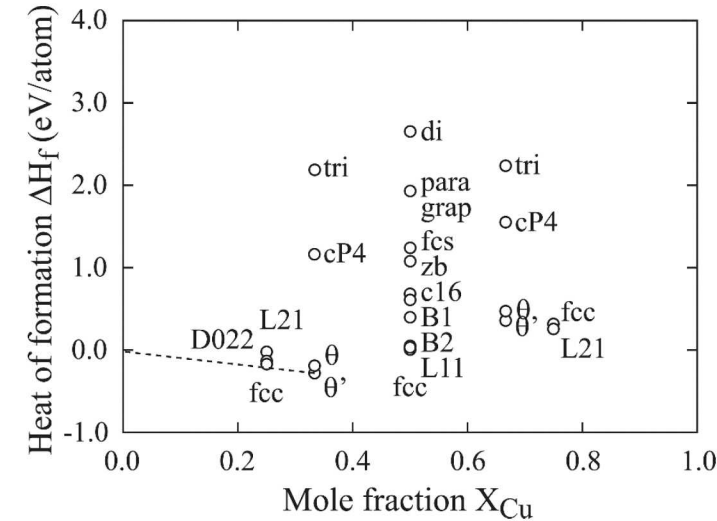
(a) Cohesive energy E_c



(b) Atomic volume Ω



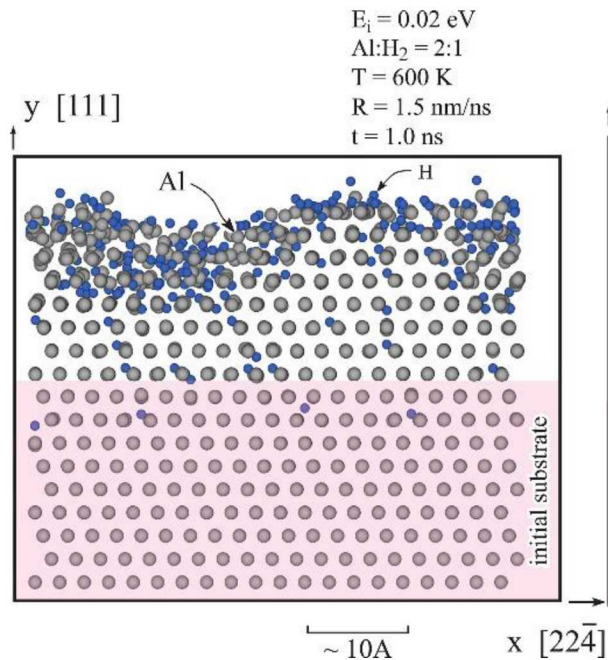
Al-Cu



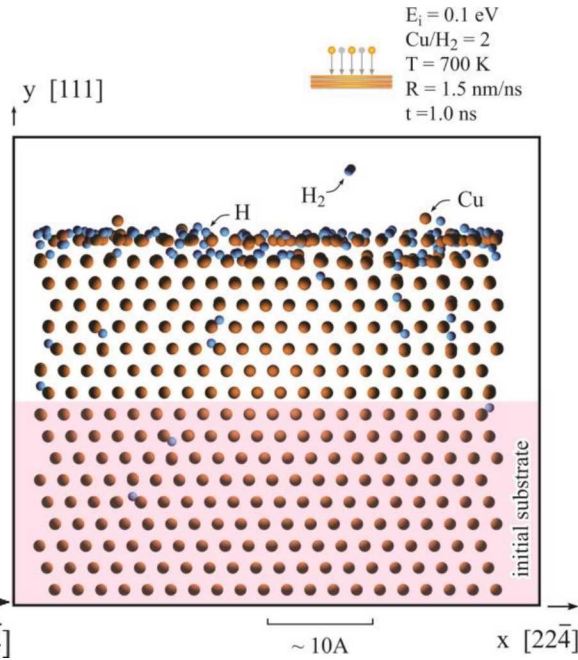
1. Energy and volume trends by potential matches well with those by DFT
2. Heat of solution supports stabilities of θ and θ' Al_2Cu phases

Stringent Validation: Growth Simulations

Al Growth

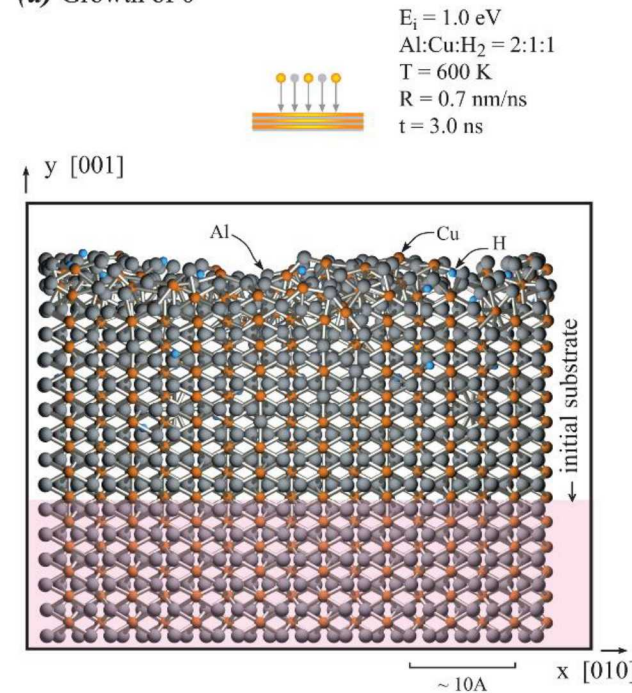


Cu Growth

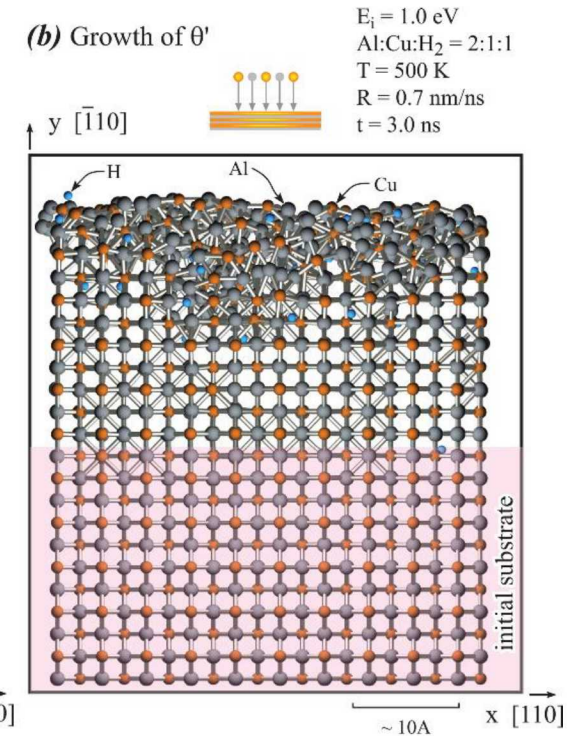


Al₂Cu Growth

(a) Growth of θ



(b) Growth of θ'



1. Crystalline growth is achieved for all possible cases
2. This strongly validates that the θ and θ' Al₂Cu phases are indeed stable



Comparison of Numerical Properties I

Lattice constants a and c or bond length d (Å), cohesive energy E_c (eV/atom), elastic constants C_{ij} (GPa), stacking fault energy γ_{sf} (mJ/m²), surface energies $\gamma_{(hkl)}$ (mJ/m²), melting temperature T_m (K), vacancy formation energy E_v (eV), interstitial formation energy E_i (eV)

Phase	Method	a, c or d		E_c	C_{ij}					γ_{sf}	$\gamma_{(hkl)}$			T_m	E_v	E_i
		a or d	c		C_{11}	C_{12}	C_{44}	C_{33}	C_{13}		$\gamma_{(100)}$	$\gamma_{(110)}$	$\gamma_{(111)}$			
Al-fcc	BOP	4.050	---	-3.361	115	63	32	---	---	133	979	1069	850	947	0.97	---
	Exp.	4.050	---	-3.361	114	62	32	---	---	120-144	980-1140		933	0.68	---	
Cu-fcc	BOP	3.615	---	-3.473	176	125	82	---	---	37	1814	1948	1570	1390	1.26	2.42
	Exp.	3.615	---	-3.473	176	125	82	---	---	45	1790		1358	1.27	2.8-4.2	
H ₂	BOP	0.752	---	-2.247	---	---	---	---	---	---	---	---	---	---	---	---
	QM	0.752	---	---	---	---	---	---	---	---	---	---	---	---	---	---
	Exp.	---	---	-2.247	---	---	---	---	---	---	---	---	---	---	---	---
AlCu ₂ - θ	BOP	6.151	4.635	-3.588	113	49	27	128	73	---	---	---	---	---	---	---
	Exp.	6.052	4.878	-3.590	186	72	29	179	79	---	---	---	---	---	---	---
AlCu ₂ - θ'	BOP	5.720	5.706	-3.677	134	54	24	---	---	---	---	---	---	---	---	---
	DFT	5.755	5.755	-3.869	179	64	80*	---	---	---	---	---	---	---	---	---



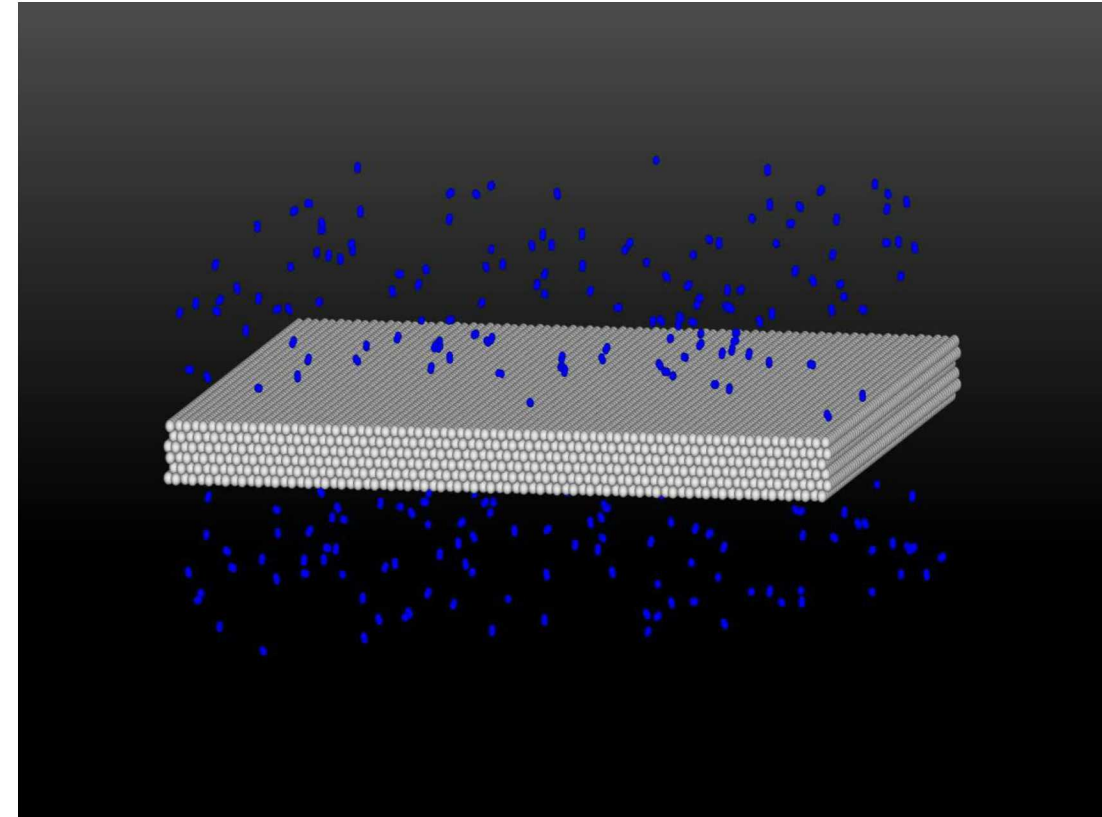
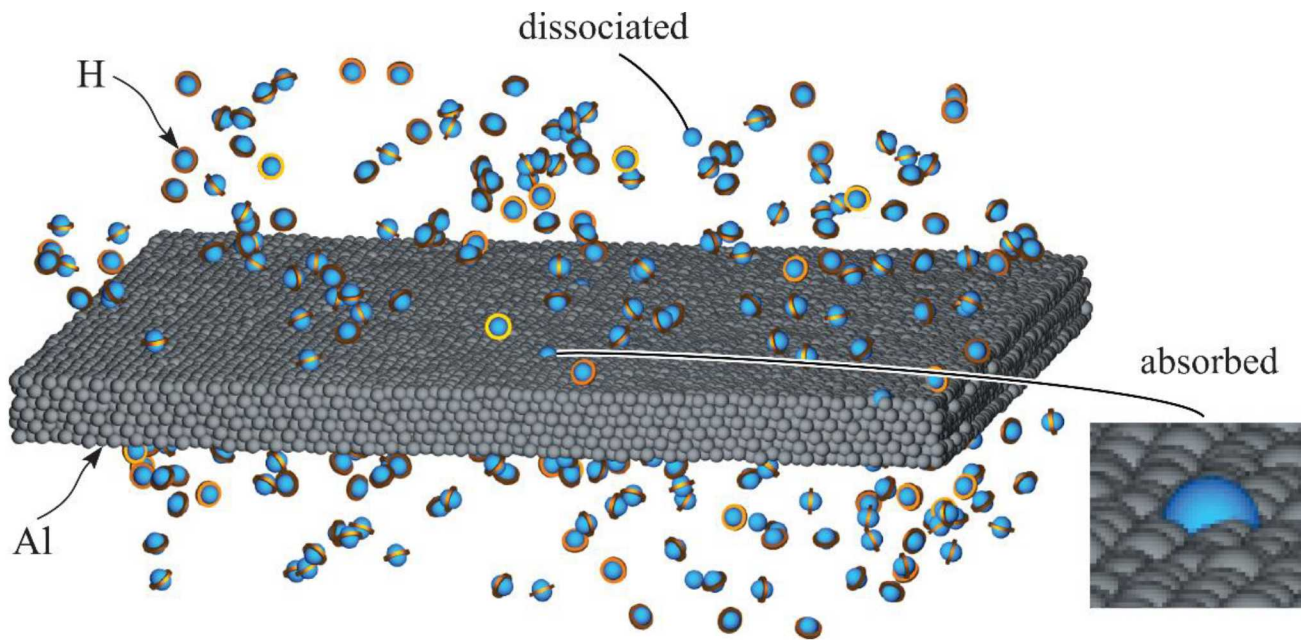
Comparison of Numerical Properties II

Cohesive energy E_c (eV/atom) and atomic volume Ω (\AA^3)

	BOP		DFT (scaled)		DFT (original)		Exp.		ADP
	E_c	Ω	E_c	Ω	E_c	Ω	E_c	Ω	E_c
Al-fcc	-3.3611	16.6012	-3.3600	16.6077	-3.6107	16.4165	-3.360	16.60	-3.36
AlH _{0.25,T}	-2.9644	14.7945	-3.0736	14.0834	-3.2543	13.9534	-----	-----	-----
AlH _{0.25,O}	-2.9117	14.2328	-3.0417	13.8198	-3.2206	13.6922	-----	-----	-----
AlH-zb	-2.4987	12.3872	-2.5839	10.5406	-2.6768	10.4795	-----	-----	-1.96
AlH-wz	-2.4992	12.3507	-2.5788	10.5481	-2.6716	10.4870	-----	-----	-----
AlH-B1	-2.4342	9.5403	-2.5605	9.4615	-2.6526	9.4067	-----	-----	-1.88
AlH-gra	-2.4141	11.3986	-2.5522	10.6369	-2.6440	10.5753	-----	-----	-----
AlH ₂ -rut	-2.3665	11.0654	-2.5414	9.6267	-2.6017	9.5895	-----	-----	-1.53
AlH ₂ -q'	-2.3601	9.6026	-2.5186	8.1865	-2.5783	8.1549	-----	-----	-----
H ₂ -di	-2.2468	-----	-2.4828	-----	-2.4828	-----	-2.247	-----	-2.373
AlH-B2	-2.2695	8.5718	-2.1624	10.0266	-2.2402	9.9686	-----	-----	-1.58
AlH-fcs	-2.0584	-----	-2.1032	-----	-2.1788	-----	-----	-----	-----
AlH-grap	-2.0652	-----	-2.5046	-----	-2.1285	-----	-----	-----	-----
(AlH) ₂ -para	-1.4922	-----	-1.9605	-----	-2.0310	-----	-----	-----	-----
Al ₃ H-tet	-1.1323	-----	-1.7344	-----	-1.8297	-----	-----	-----	-----
AlH ₂ -tri	-1.4979	-----	-1.6464	-----	-1.6854	-----	-----	-----	-----
AlH-di	-1.0814	-----	-1.6058	-----	-1.6635	-----	-----	-----	-----
Al ₂ H-tri	-1.1806	-----	-1.5583	-----	-1.6340	-----	-----	-----	-----



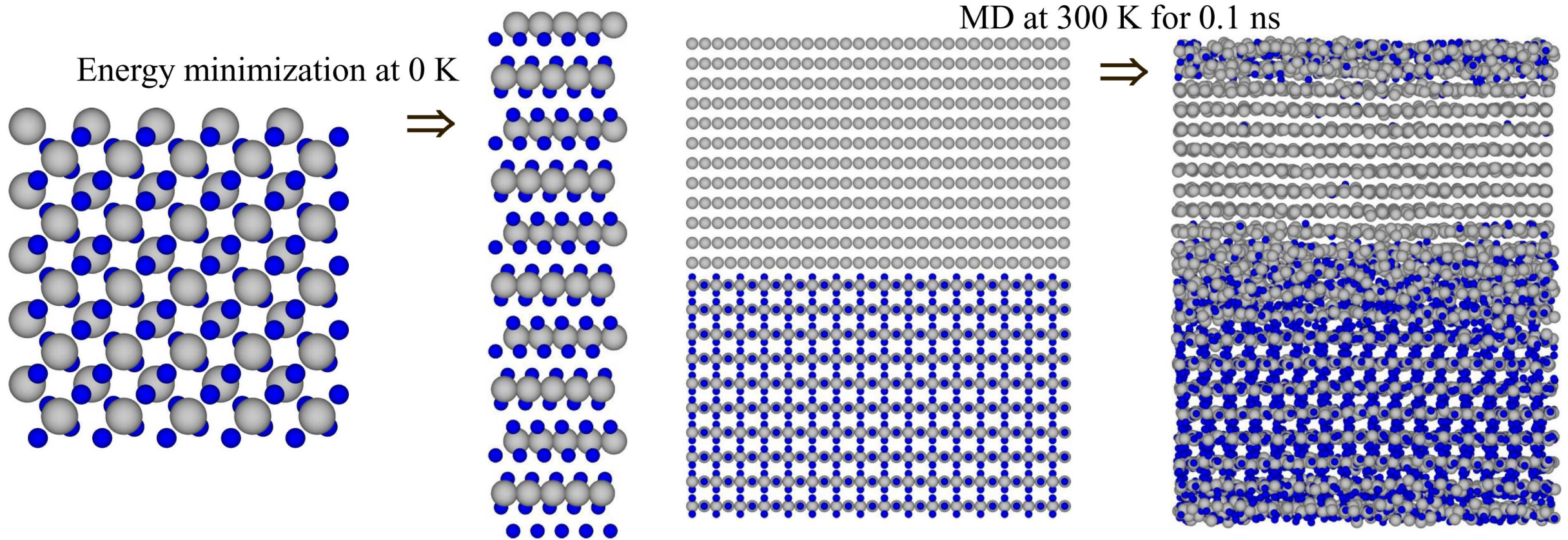
MD Simulation of H₂ Absorption



Such simulations are not possible without capturing the $\text{H} + \text{H}_2 \rightleftharpoons \text{H}_2 + \text{H}$ reaction.



Literature Mg-H Potentials



Simulation using the literature Mg-H **EAM** potential
(Ruda et al, ANALES DE LA ASOCIACION
QUIMICA ARGENTINA, 84, 393, 1996)

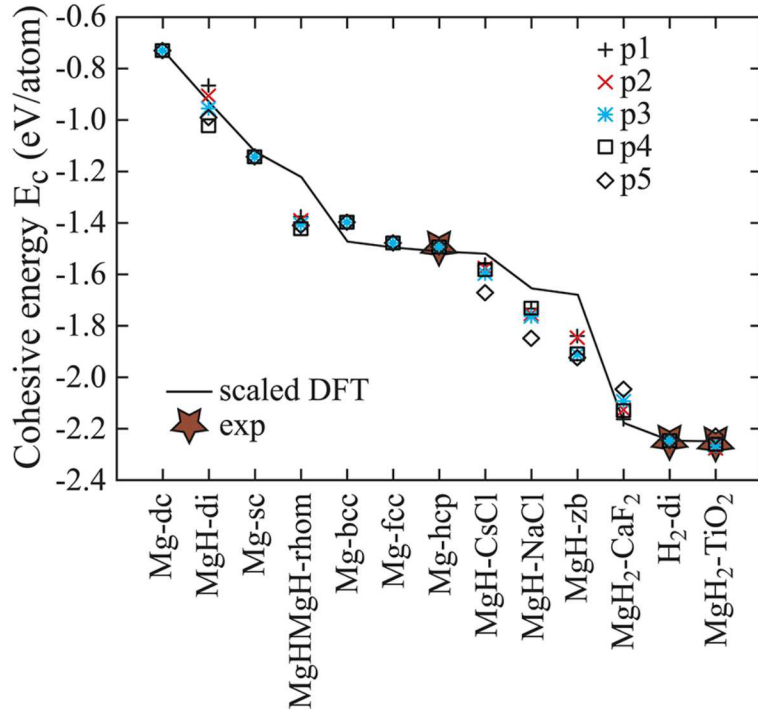
Simulation using the literature Mg-H **ReaxFF** potential
(S. Cheung, W. Q. Deng, A. C. T. van Duin, W. A.
Goddard, J. Phys. Chem., 109, 851 2005)



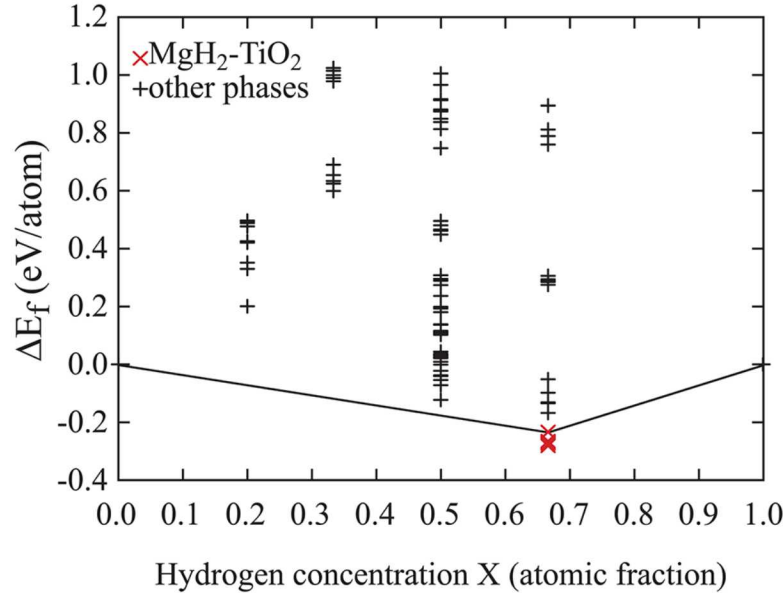
Property Trends

Energy Trends

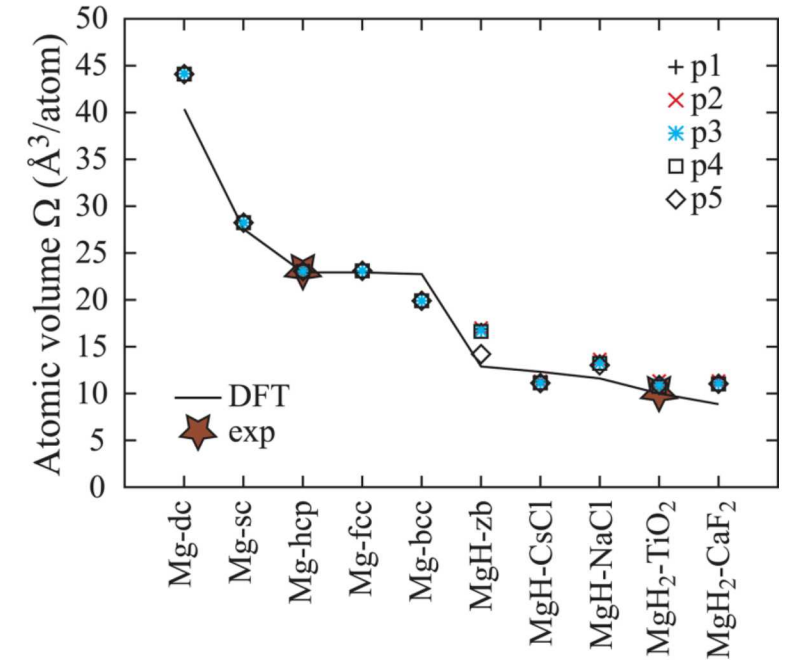
(a) Cohesive energy E_c



(b) Heat of formation ΔE_f from all potentials



Volume Trends



Mg-hcp Elastic Constants

Table I. Elastic constants C_{11} , C_{33} , C_{44} , C_{13} , and bulk modulus $B = (2C_{11} + 2C_{12} + C_{33} + 4C_{13})/9$ in unit $\text{eV}/\text{\AA}^3$.

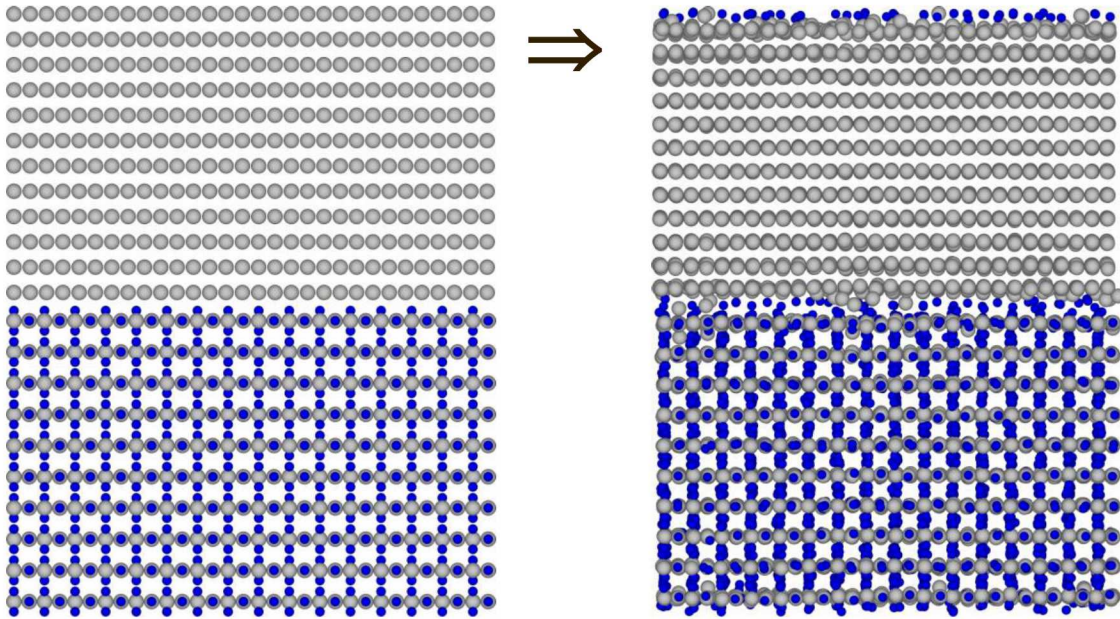
C_{11}		C_{33}		C_{44}		C_{13}		B	
Cal.	Exp.	Cal.	Exp.	Cal.	Exp.	Cal.	Exp.	Cal.	Exp.
0.40	0.40	0.42	0.41	0.11	0.12	0.14	0.14	0.23	0.23

Our Mg-H potential seems to captures the property trends of important phases well



Stringent MD Tests

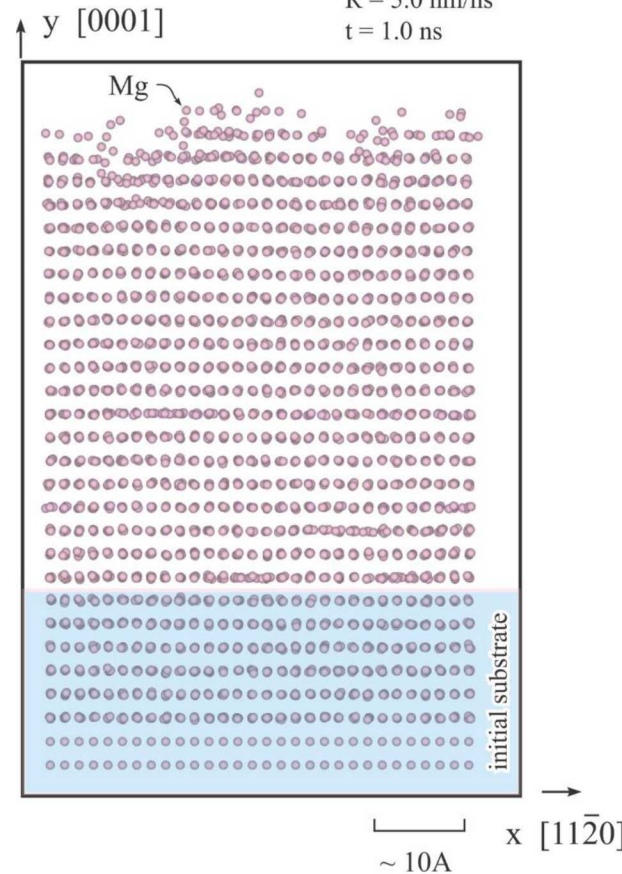
MD at 300 K for 1.0 ns



Our Mg-H potential passes perhaps the most stringent MD tests about stability

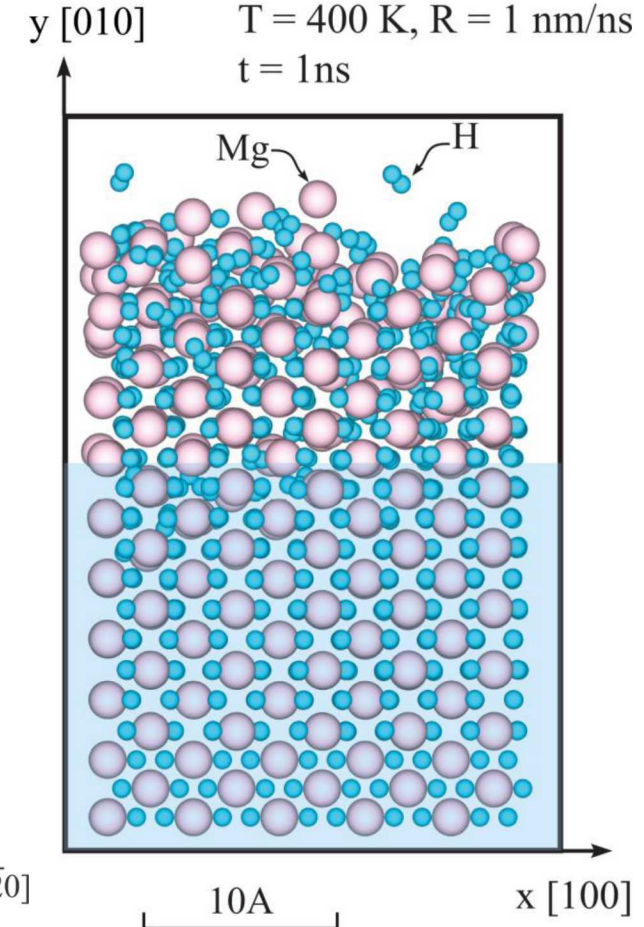
Mg-hcp Growth

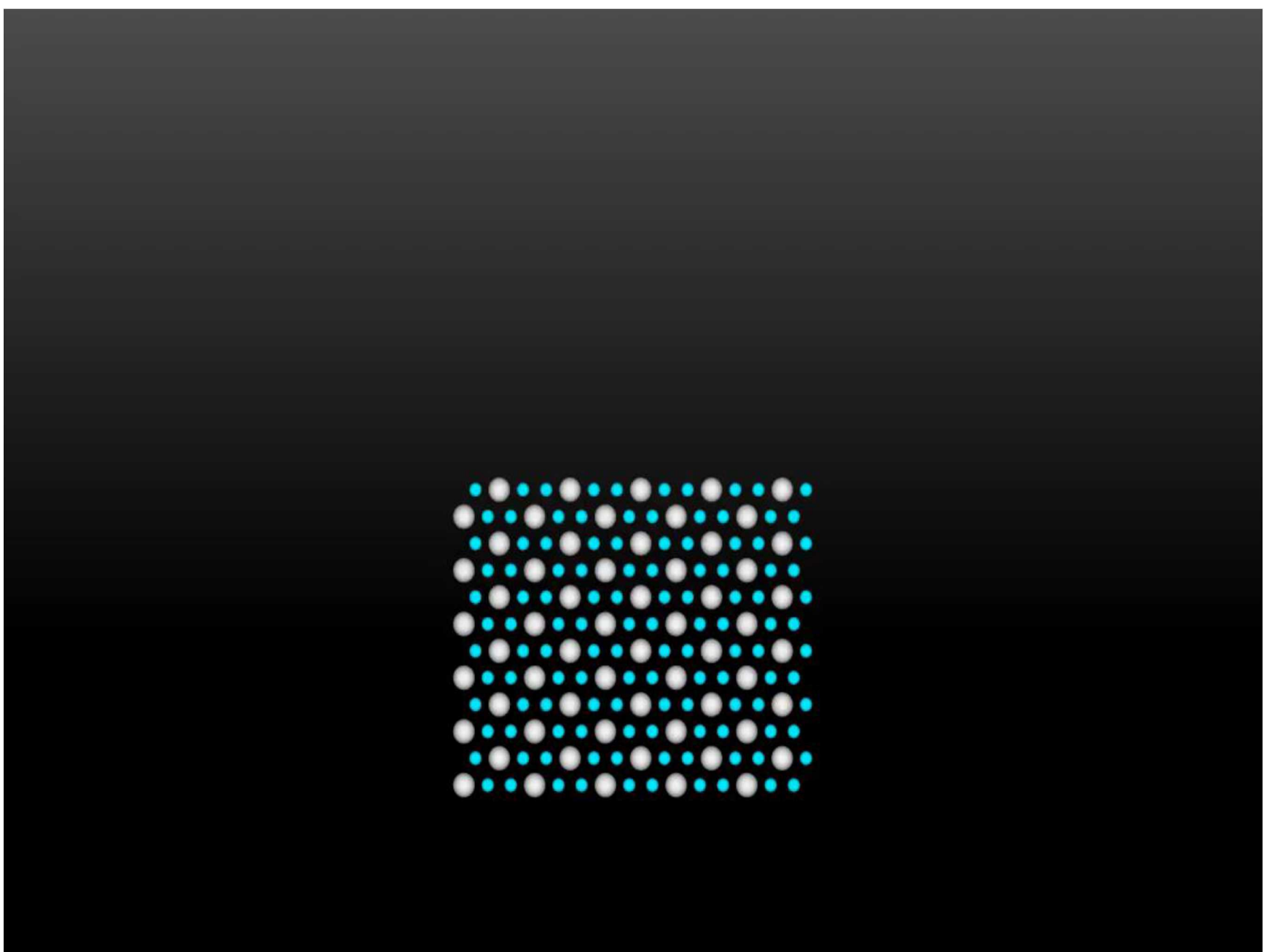
$E_i = 0.5$ eV
 $T = 300$ K
 $R = 5.0$ nm/ns
 $t = 1.0$ ns



MgH₂-Rutile Growth

$H/Mg = 4$, $E_i = 0.1$ eV
 $T = 400$ K, $R = 1$ nm/ns
 $t = 1$ ns





Conclusions

1. In general, if MD problems can be represented by periodic boundary conditions, then statistical errors can always be reduced to near zero without time/length scale issues
2. Our Al-Cu-H and Mg-H bond order potentials seem to be satisfactory for reactive simulations

